LUND UNIVERSITY

Real-time method for fitting time-resolved reflectance and transmittance measurements with a Monte Carlo model

Pifferi, A; Taroni, P; Valentini, G; Andersson-Engels, Stefan

[Link to publication]

Real-time method for fitting time-resolved reflectance and transmittance measurements with a Monte Carlo model

Antonio Pifferi, Paola Taroni, Gianluca Valentini, and Stefan Andersson-Engels

An efficient method is proposed for the evaluation of the absorption and the transport scattering coefficients from a time-resolved reflectance or transmittance distribution. The procedure is based on a library of Monte Carlo simulations and is fast enough to be used in a nonlinear fitting algorithm. Tests performed against both Monte Carlo simulations and experimental measurements on tissue phantoms show that the results are significantly better than those obtained by fitting the data with the diffusion approximation, especially for low values of the scattering coefficient. The method requires an *a priori* assumption on the value of the anisotropy factor *g*. Nonetheless, the transport scattering coefficient is rather independent of the exact knowledge of the *g* value within the range $0.7 < g < 0.9$. © 1998 Optical Society of America

OCIS codes: 170.6510, 300.6500, 290.7050.

1. Introduction

The knowledge of the optical properties of biological tissues is of great interest for clinical diagnostics as well as for the optimization of therapeutic protocols. Among the techniques under study, time-resolved remittance spectroscopy (either reflectance or transmittance) proved particularly appealing, since it allows the noninvasive evaluation of the absorption (μ_a) and transport scattering (μ_s') coefficients.[1–3] The diffusion approximation to the radiative transport equation has been successfully used to fit time-resolved data obtained for long interfiber distances ($\rho > 1$ cm) in highly scattering media ($\mu_s' > 20$ cm^{-1}),[4,5] as it provides a good description of the photon migration after a long path in the medium. However, the diffusion equation fails to predict the initial events of photon migration,[6–8] and other models should be considered.

Very recently, interest has grown in the possibility of using a Monte Carlo code to interpret photon-migration curves. In the case of a cw measurement, the value of μ_a, the scattering coefficient μ_s, and the anisotropy factor (mean cosine of the scattering angle for one scattering event) g can be inferred from a lookup table of Monte Carlo simulations of the diffuse reflectance and total and collimated transmittance through a turbid slab.[9] Another approach has been proposed for the analysis of coherent backscattered photon distributions. A single Monte Carlo simulation is performed, and the individual photon histories recorded. The photon angular distribution corresponding to any combination of the scattering and the absorption coefficients is then reconstructed from the database of photon histories, applying the Beer–Lambert factor to account for the absorption and a proper scaling factor to account for the scattering.[10]

In the case of a time-resolved measurement, the previous solution is not effective since a high number of individual photon histories must be processed to yield a statistically significant output curve. Kienle and Patterson[11] and, independently, the authors[12] have proposed a fast procedure for the construction of a time-resolved reflectance distribution. The key idea in Ref. 12 is to start from a library of simulated photon distributions obtained for a set of different scattering coefficients and null absorption. The pho-

ton time distribution corresponding to any value of μ_a and $\mu_s{}'$ is then calculated when the two nearest curves in the library are interpolated and the Beer–Lambert law is applied. This procedure is quite fast and can easily be implemented in a fitting algorithm for the evaluation of the optical properties. The major differences between the methods proposed in Refs. 11 and 12 are addressed in Section 6.

Here we extend the method to include also time-resolved transmittance curves. Moreover, we check the accuracy of the procedure by evaluating experimental results, since up to now, to the best of our knowledge, the method has been tested only on simulations,[11,12] and its validity for real experiments still has to be proved. Time-resolved transmittance measurements were performed on tissue phantoms covering a wide range of optical properties. In these measurements a Ti:Sapphire laser was used as a source and a synchroscan streak camera was used for the detection. The experimental curves were analyzed both with the proposed Monte Carlo method and with a standard solution of the diffusion equation. The results were also compared with the test performed on simulations for the same set of optical properties. Finally, tests on simulations were carried out also for the reflectance case.

2. Theory

In this section, we present a method to obtain the time distribution $R(\mu_s, \mu_a, \rho, t)$ of diffusely reflected light as a function of time t at the surface of a turbid medium at a distance ρ from the injection point. We used a cylindrical coordinate system with light incident as a short pulse in the origin, and exploited some general properties of time-resolved reflectance curves that, although well known, are recalled to appreciate the limits of the method and some interesting implications. The results are then extended to the evaluation of the time-resolved transmittance $T(\mu_s, \mu_a, \rho, d, t)$ through a slab of thickness d.

We assume that the medium is (i) semi-infinite, (ii) homogeneous, and (iii) continuous. Moreover, we assume that we know the values of the refraction index n and of the anisotropy factor g of the medium.

The first step consists of splitting the effects of absorption and scattering. Let us first suppose that we know the reflectance function $R(\mu_{s0}, \mu_a = 0, \rho, t)$ for a nonabsorbing white medium with a certain scattering coefficient μ_{s0}.

Furthermore, we use the fact that it is the scattering properties that determine the photon path. The scattering coefficient influences the length of the free path between two subsequent interactions, whereas the angular deviation of the photon is ruled by the anisotropy factor g. Therefore, if μ_{s0} is multiplied by a factor k, the shape of the path will be unaffected, whereas the length of each step will be divided by the factor k (as shown in Fig. 1). Thus one can derive the reflectance function for other μ_s values by scaling R for μ_{s0} by the factor $k = \mu_s/\mu_{s0}$:

$$R(\mu_s, \mu_a = 0, \rho, t) = k^3 R(\mu_{s0}, \mu_a = 0, k\rho, kt), \quad (1)$$
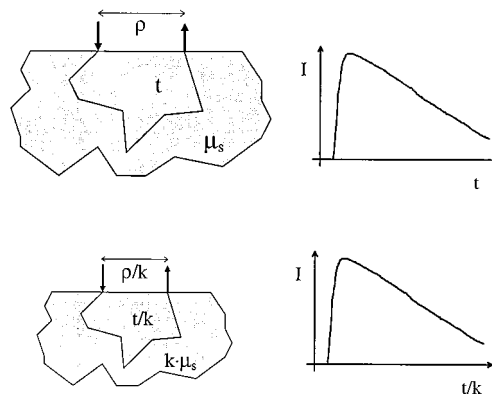

Fig. 1. Scattering coefficient determines the distance between two scattering sites, whereas the shape of the photon path is fixed solely by the g value. The TPSF of a medium with a certain μ_s can be derived when the TPSF of a medium with a different μ_s is scaled and if both are characterized by the same g value.

if both situations are characterized by the same g value.

Although the absorption simply selects the photons that ultimately survive, as illustrated in Fig. 2, it cannot alter the photon path. Therefore, if some absorption is added to this medium, the corresponding reflectance function can be derived from Eq. (1) with the Beer–Lambert law. The diffuse reflectance function can thus be expressed

$$R(\mu_s, \mu_a, \rho, t) = k^3 R(\mu_{s0}, \mu_a = 0, k\rho, kt)\exp(-\mu_a vt), \quad (2)$$

where $v = c/n$ is the speed of light in the medium. This approach is the same as used, for example, in the random-walk model,[13] and it has a general applicability, regardless of the theoretical model considered, as long as the hypotheses of the homogeneous and the continuous medium are satisfied.

By utilizing the relations in Eqs. (1) and (2), one can construct the distribution $R(\mu_s, \mu_a, \rho, t)$ for every set of optical coefficients starting from the single Monte Carlo simulation of a nonabsorbing medium
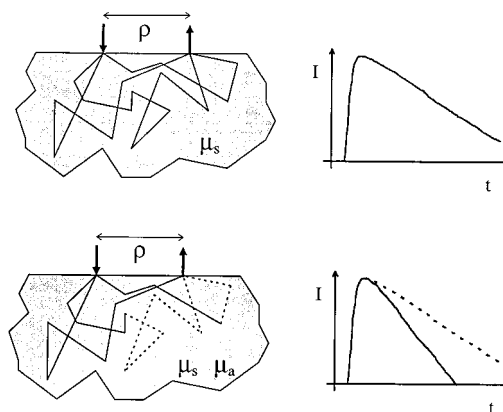

Fig. 2. Absorption coefficient reduces the survival probability of photons for elapsing time. The TPSF of photons reemitted from a turbid medium can be derived when the TPSF of a medium with the same scattering and no absorption is weighed.

with a certain scattering μ_{s0}. Nevertheless, to be able to apply the scaling factor for any value of μ_s, without any other approximation, one must record and process all the individual histories of photons. Since a high number of photons is needed to build a time-resolved curve with good statistics, the calculation of a temporal point spread function (TPSF) for a given set of optical properties can still be too time consuming to be effectively used in an iterative fitting procedure.

We followed an alternative approach, introducing a further approximation. First, we built a library of time-resolved reflectance curves for white media with a set of different scattering coefficients, processed all the photon records of a unique Monte Carlo simulation, and applied Eq. (1). We followed this procedure only once to buildup the library for a certain geometry. The curve produced by an arbitrary μ_s can be obtained from the linear interpolation of the two library curves corresponding to the scattering coefficients μ_{s1} and μ_{s2} nearest to μ_s (with $\mu_{s1} < \mu_s < \mu_{s2}$). Then, we took into account the effect of the absorption by applying the exponential factor, as shown in Eq. (2). Clearly, this procedure introduces an intrinsic approximation in the model related to the finesse of the library.

This method can also be used to evaluate a time-resolved transmittance distribution. In this case, we consider a pulse of light normally incident on the surface of a slab of thickness d, and we are interested in the time distribution $T(\mu_s, \mu_a, d, \rho, t)$ of the light reemitted on the opposite side of the slab. Clearly, in this geometry, the hypothesis (i) of the semi-infinite medium is no longer valid, and it is not possible to scale the scattering coefficient as in Eq. (1). Therefore, compared with the reflectance case, the building of the library takes longer, since curves for different scattering coefficients must be simulated independently. Nevertheless, once the library is available, the reconstruction of the transmission curve requires the same computer time as for the reflectance case. Generally speaking, hypothesis (i) allows an easier building of the library, but it is not strictly necessary. The other tools, that is, the linear interpolation and the Beer–Lambert factor to account for the absorption, can be used in any geometry.

In the beginning, we supposed that we knew the value of the anisotropy factor g and that it was the same for the library curves as well as for the experimental data to be fitted. This requirement is hard to fulfill in a real situation, since the measurement of g is generally difficult and g can vary among different biologic samples. Moreover, it is not practical to build a different library for every possible g. Nevertheless, in many instances, the optical parameter of interest is the transport scattering coefficient $\mu_s' = \mu_s(1 - g)$. Therefore a small indeterminacy in the g value could be acceptable as long as the corresponding variation on the fitted μ_s' value can be neglected. This aspect is addressed in the Subsection 3.A.

It is useful to check the accuracy of the proposed Monte Carlo evaluation method in fitting a TPSF to extract the optical properties of turbid media against that provided by other models. This makes it possible to compare the performances of the different methods. In particular, we consider the diffusion approximation to the radiative transport theory, which is widely used to evaluate the optical properties of turbid media.

In the case of a semi-infinite homogeneous continuous medium [i.e., hypotheses (i) to (iii)], the solution for the reflected light, reemitted at a distance ρ, is given by[1]:

$$R(\rho, t) = (4\pi Dc/n)^{-3/2} z_o t^{-5/2}$$
$$\times \exp(-\mu_a ct/n)\exp\left(-\frac{\rho^2 + z_o^2}{4Dct/n}\right), \quad (3)$$

where $z_0 \cong (\mu_s')^{-1}$ and $D = [3(\mu_s' + \mu_a)]^{-1}$. This expression was derived with the use of the zero-boundary condition, i.e., the assumption that the fluence rate is null on the surface.

In the diffusion approximation, the expression of the transmittance through a homogeneous continuous slab of thickness d is given by[1]:

$$T(\rho, d, t) = (4\pi Dct/n)^{-3/2} t^{-5/2}$$
$$\times \exp(-\mu_a vt)\exp\left(-\frac{\rho^2}{4Dct/n}\right)$$
$$\times \sum_{n=1, k=2n-1}^{n=\infty} \left\{ (kd - z_0)\exp\left[\frac{-(kd - z_0)^2}{4Dct/n}\right] \right.$$
$$\left. - (kd + z_0)\exp\left[\frac{-(kd + z_0)^2}{4Dct/n}\right] \right\}, \quad (4)$$

where ρ is the distance between the collection point and the direction of incidence. For practical applications related to photon propagation in biologic media, the summation in Eq. (4) can be truncated at the first two dipoles ($n = 1$), since higher-order terms yield negligible contributions.

In this study, we assumed a different expression for the diffusion coefficient: $D = (3\mu_s')^{-1}$, independent of μ_a. In the derivation by Furutzu and Yamada,[14] they assert that this expression is more appropriate than the one normally used. The lack of dependence on μ_a is also in agreement with the analysis above, as Eq. (2) holds for any theoretical model under the stated hypotheses. Since the information on μ_a is carried exclusively by the factor $\exp(-\mu_a vt)$, the diffusion coefficient must be exactly the same as for a white medium with $\mu_a = 0$. In practice, since the diffusion approximation is valid only if $\mu_s' \gg \mu_a$, the numerical difference between the two expressions is expected to be small whenever the diffusion equation holds true. However, since the new expression for D is not yet universally accepted, we also performed tests to analyze the simulated and the experimental data and used the conventional expression for $D = [3(\mu_s' + \mu_a)]^{-1}$ in Eqs. (3) and (4). The corresponding discrepancy in the fitted values of μ_a or μ_s' in
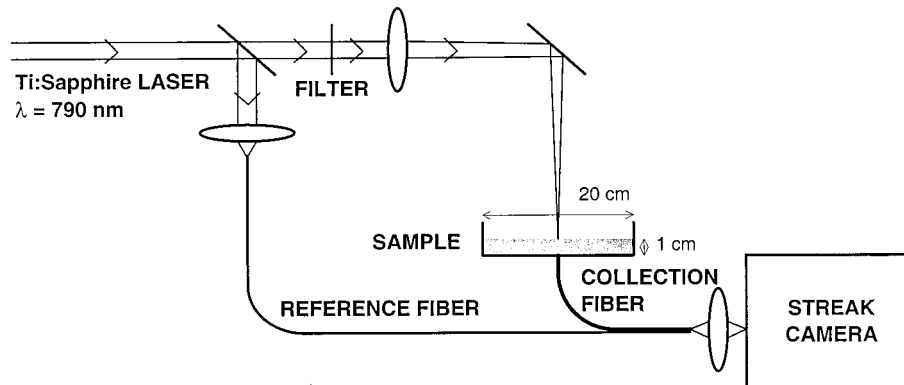
Fig. 3.   Experimental setup for the time-resolved transmittance measurements on tissue phantoms.

which the two expressions for D were used, was found to be much smaller than the error due to the model itself. Therefore only results obtained with $D = (3\mu_s')^{-1}$ are presented in the following sections.

3. Materials and Methods

A. Simulations

The library curves and the test simulation curves were produced with a standard Monte Carlo code[15] modified for temporal applications.[16] For both reflectance and transmittance, the corresponding libraries were built with simulated data corresponding to 12 different values of μ_s', starting from 1.0 cm^{-1} and scaled in a geometric progression of ratio $\sqrt{2}$ (i.e., 1.0, 1.4, 2.0, 2.8, 4.0, 5.7, 8.0, 11.3, 16.0, 22.6, 32.0, and 45.3 cm^{-1}). When we followed the description in Section 2, in the case of reflectance, all the curves were obtained from a single simulation of 10 million photons. In the case of transmittance, all the library curves were simulated independently, with 10 million photons each, since the scaling factor was not applicable.

To test the validity of the proposed method, we simulated a total of 25 test reflectance curves and 25 transmittance curves, combining 5 different transport scattering coefficients ($\mu_s' = 1.5, 3.0, 6.0, 12$, and 24 cm^{-1}) and 5 absorption coefficients ($\mu_a = 0.1, 0.2, 0.4, 0.8$, and 1.6 cm^{-1}), always with an interfiber distance $\rho = 1.0$ cm (reflectance) or a slab thickness $d = 1.0$ cm and $\rho = 0.0$ cm (transmittance). We obtained each of the test curves from simulations of at least 1 million injected photons.

For both the library and the test curves, the values of $g = 0.80$ and $n = 1.33$ were assumed. Moreover, to evaluate the effect of an incorrect knowledge of the g value, we simulated two more sets of test reflectance curves, which corresponded to $g = 0.70$ and $g = 0.90$. The values of the scattering coefficient μ_s were chosen so as to yield the same values of μ_s' as in the set of curves with $g = 0.80$.

B. Experiments

The transmittance measurements were performed on phantoms composed of water solutions of Intralipid

(Pharmacia) and black ink (Pelikan) by using a mode-locked Ti:Sapphire laser (Coherent, Model Mira 900) and a streak camera (Hamamatsu, Model C1587), as shown in Fig. 3. The phantom solution was poured into a glass tank, 20 cm $\times$ 20 cm wide, in proper amount to form a 1.0-cm-thick slab. The laser was tuned at 790 nm with a pulse duration of $\approx$100 fs. The laser beam was focused on the upper surface of the phantom and the light emitted at the lower surface was collected by a 600-μm quartz fiber. The light was then focused on the entrance slit of the streak camera, which was running in synchroscan mode. A small fraction of the laser beam was coupled to a 200-μm quartz fiber and directly fed into the streak camera to account for eventual time drifts of the instrumentation. The instrumental transfer function, measured with the same setup without any solution in the tank, showed a FWHM $<$ 30 ps.

The optical properties of Intralipid and black ink were characterized performing a time-resolved reflectance measurement with an interfiber distance $\rho = 1.4$ cm on a water solution containing 3×10^{-2} (solid fraction) Intralipid and 2×10^{-5} (v/v) ink. Under these conditions, the measurement can be safely analyzed with the diffusion expression [Eq. (4)].[5] We obtained values corresponding to $\mu_s' = 160$ cm^{-1} for the batch solution of 20% Intralipid and $\mu_a = 4.1 \times 10^4$ cm^{-1} for the pure ink. This preliminary characterization was exploited to produce a total of 25 solutions with known optical properties, combining 5 values of μ_s' (1.5, 3.0, 6.0, 12, and 24 cm^{-1}) with 5 values of μ_a (0.1, 0.2, 0.4, 0.8, and 1.6 cm^{-1}).

C. Fitting Procedure and Data Analysis

The simulated curves were directly fitted to the analytical solution of the diffusion equation or evaluated with the suggested Monte Carlo method. The experimental curves were analyzed in the same way. In this case however, both the theoretical curves and the simulated library curves were first convoluted with the instrumental transfer function before the evaluation. In the case of transmittance measurements, the delay introduced by the glass wall of the tank was accounted for in the diffusion equation, and the Monte Carlo library was built for a two-layered

medium (liquid phantom-glass). For both simulated and experimental data, the range of the fit included all the points in the curve over a fixed threshold. In particular, the threshold was set to 2% of the peak value on the tail of the curve, whereas two different thresholds of 2% and 80% were tested for the leading edge. To achieve a faster and more robust fitting procedure, we fixed the amplitude by normalizing the theoretical curves to the area of the test curves and by varying only two parameters, μ_a and μ_s'. The fitting procedure was developed with the Microsoft Excel Solver routine for nonlinear optimization.[17] The best fit was obtained by minimizing the reduced χ^2.

The reconstruction of the theoretical expression (for both the diffusion and the Monte Carlo models) as well as the convolution procedure were compiled in a dynamic-link library, written in C, for computational efficiency. The time needed to reconstruct a curve was almost the same with both models and was negligible compared with the convolution process. A fit with the diffusion model takes typically 4 s on a standard Intel 486DX2, 66 MHz personal computer. The Monte Carlo model requires 8 s of computer time, owing to the higher number of iterations needed for convergence.

The accuracy of both models in fitting either the simulated or the experimental curves was evaluated in terms of the relative error ε, defined as

$$\varepsilon = \frac{|\mu_f - \mu_e|}{\mu_e}, \qquad (5)$$

where μ_e is the effective value (of μ_a or μ_s') used in the simulations or calculated from the characterization of the samples, whereas μ_f is the corresponding fitted value.

4. Test against Simulations

In a first step, we evaluated the algorithm to extract the optical properties of turbid media by fitting Monte Carlo-simulated diffuse reflectance or transmittance curves and by comparing the fitted optical properties to the ones used for the simulations. Figure 4 shows the pattern of the relative error for the fitting of μ_a with reflectance and transmittance curves [Figs. 4(a)–4(c) and Figs. 4(d)–4(f), respectively] with either the diffusion expression or the Monte Carlo method. For the Monte Carlo, we used only the wider fitting range [Figs. 4(a) and 4(d)], whereas for the diffusion, which is not adequate to predict photon propagation at early times,[6] we tested both ranges, setting the first threshold on the remittance curve to 2% [Figs. 4(b) and 4(e)] and 80% [Figs. 4(c) and 4(f)] of the peak value, respectively. The error is expressed as a function of the optical properties considered in the simulations and represented in contour plots. Bilinear interpolation was performed on the 25 values of ε, and areas of the plane (μ_a, μ_s') in which the error falls within different selected intervals were displayed with different shades: $\varepsilon < 10\%$, white; $10\% < \varepsilon < 20\%$, light gray; $20\% < \varepsilon < 30\%$, dark gray; and $\varepsilon > 30\%$, black, for both reflectance
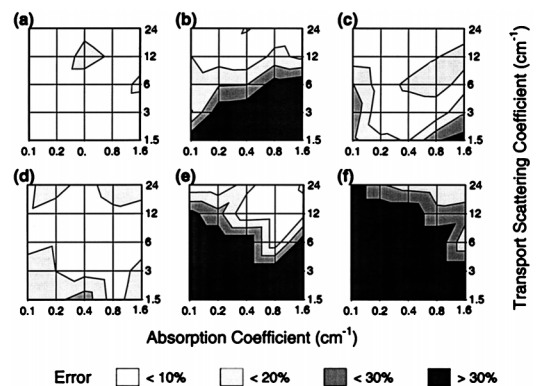

Fig. 4. Relative error on the fitted μ_a for (a)–(c) simulated reflectance or (d)–(f) transmittance curves. The method used for the fitting is (a) and (d) the Monte Carlo, (b) and (e) the diffusion with the full fitting range, or (c) and (f) the diffusion with the reduced fitting range.

and transmittance measurements. The Monte Carlo method can be successfully used to fit the curves with an error generally $<10\%$ for all the optical parameters tested. As clearly illustrated in Fig. 4, fits with the wider range with the diffusion approximation solution results in more inaccurate estimations of the optical properties, yielding ε values $>30\%$ for $\mu_s' < 10$–15 cm^{-1}. The behavior is drastically improved, but only in reflectance, if a large part of the leading edge of the curves is disregarded. In fact, in this case, the error is $<10\%$ for most of the optical coefficients considered. On the contrary, for transmittance measurements, the estimated values become even more inaccurate when the reduced fitting range is used.

Figure 5 shows the corresponding relative error obtained for μ_s'. Again, the Monte Carlo method provides accurate results with an error mostly $<10\%$ for all combinations of optical properties studied both in reflectance and in transmittance [Figs. 5(a) and 5(d)]. The diffusion model is clearly less adequate to evaluate the scattering properties with high accuracy
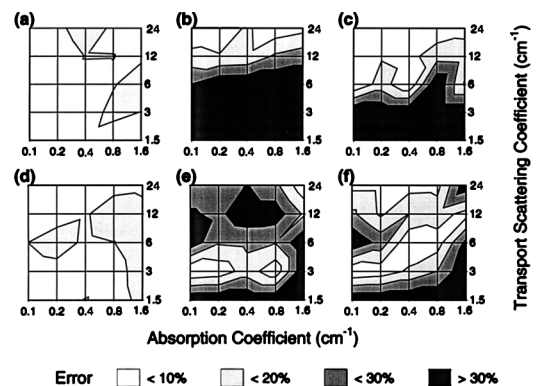

Fig. 5. Relative error on the fitted μ_s' for (a)–(c) simulated reflectance or (d)–(f) transmittance curves. The method used for the fitting is (a) and (d) the Monte Carlo, (b) and (e) the diffusion with the full fitting range, or (c) and (f) the diffusion with the reduced fitting range.
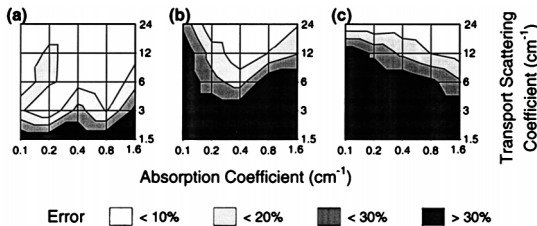
Fig. 6. Relative error on the fitted μ_a for experimental transmittance curves for which (a) the Monte Carlo, (b) the diffusion with the full fitting range, or (c) the diffusion with the reduced fitting range were used.

Fig. 7. Relative error on the fitted μ_s' for experimental transmittance curves for which (a) the Monte Carlo, (b) the diffusion with the full fitting range, or (c) the diffusion with the reduced fitting range were used.

for both fitting ranges considered. It may be useful to note that the error is always an overestimation of μ_s'.

In the case of reflectance measurements, additional values of the transport scattering coefficient and the interfiber distance had already been tested, and similar results were obtained.[12]

To test the dependence of the fitted values of μ_a and μ_s' on the exact knowledge of g in the Monte Carlo model, we used the same library (obtained with $g = 0.80$) to fit a set of test simulations that we produced starting from a different g value. Two values for g were tested, a lower one ($g = 0.70$) and a higher one ($g = 0.90$). In both cases, the corresponding relative error on the fitted μ_a or μ_s' was rather small, being $<10\%$ for most of the points. Therefore a limited (but for practical applications realistic) inaccuracy on the g value results in only a small error of the estimated optical parameters.

5. Test against Experiments

The ability of the Monte Carlo method to estimate the optical parameters from experimental data was tested on 25 time-resolved transmittance curves measured on phantoms with known optical properties.

Using for the fitting procedure the Monte Carlo method or the diffusion expression with the two different fitting ranges, we show in Fig. 6 the contour plot of the relative error on μ_a. The Monte Carlo method [Fig. 6(a)] provides a good estimation of μ_a with an error generally $<10\%$ for $\mu_s' > 3$–5 cm^{-1}. For lower values of μ_s', the experimental measurement is probably so close to the instrumental transfer function that we cannot extract reliable information by fitting the curve. The error in the estimation of μ_a with the diffusion equation is much higher for both fitting ranges, allowing reliable measures only for the highest scattering values ($\mu_s' > 10$–15 cm^{-1}).

The error in the estimation of μ_s' is shown in Fig. 7. The pattern is quite similar to the one observed for μ_a, and, again, use of the Monte Carlo method greatly reduces the error in the estimations of the optical parameters compared with fitting with the diffusion solution. In particular, for the Monte Carlo $\varepsilon < 10\%$ for $\mu_s' > 5$ cm^{-1} for the diffusion with the wider fitting range $\varepsilon > 30\%$ for $\mu_s' < 15$ cm^{-1}, and with the limited range, ε is mostly $>30\%$ for $\mu_s' < 5$
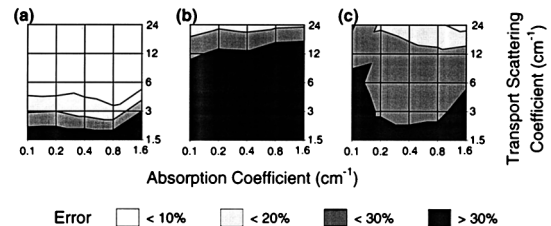
cm^{-1}, but in only a few points it reduces to values lower than 20%.

6. Discussion

With both the simulations and the measurements we aimed to explore the region where the diffusion equation is more likely to fail, that is, for a low value of the interfiber distance ($\rho \leq 1$ cm or $d \leq 1$ cm) or of the transport scattering coefficient ($\mu_s' \leq 10$ cm^{-1}). Under these conditions, the Monte Carlo method provides better results than the diffusion approximation and is adequate to evaluate the optical properties as long as the experimental curve is broad enough with respect to the instrumental transfer function. This makes the limits of good applicability somehow dependent on the performance of the particular instrumental setup used to perform the measurements. Far from these limits, that is, whenever the early events of photon migration have no crucial effect, even the diffusion equation holds safely and can be profitably used to interpret the experimental data.

The fitting method is quite insensitive to the choice of the initial values of μ_a and μ_s' for both simulated and experimental data. An initial guess of $\mu_a = 1$ cm^{-1} and $\mu_s' = 10$ cm^{-1} is appropriate for reaching the best fit in most cases. Only for very low scattering values ($\mu_s' < 3$ cm^{-1}) the lowest χ^2 was obtained, thus lowering the initial μ_s' to 1 cm^{-1}. As a general recipe, we start the fit using $\mu_s' = 10$ cm^{-1}. If the fitted μ_s' is < 4 cm^{-1}, we repeat the fit starting from $\mu_s' = 1$ cm^{-1}.

The method proposed here for generating a photon migration time distribution differs from the one presented by Kienle and Patterson.[11] In that study, the Monte Carlo code was used to simulate a unique time-resolved reflectance distribution corresponding to a fixed μ_{s0}' and a time scale τ, disregarding the information on the individual photon histories. Thus the scaling relation of Eq. (1) could be applied to produce a set of curves corresponding to discrete values of μ_s', ρ, and τ. Therefore the TPSF's corresponding to any value of μ_s', ρ, and τ were obtained when the set of reflectance curves with respect to both the radial position and the time were interpolated. We followed a different approach, building a library of Monte Carlo simulations corresponding to the desired values of ρ and τ and different values of μ_s'. Then, the TPSF was generated when the li-

brary curves were interpolated only over $\mu_s{}'$. The library curves must be tailored to the specific experimental setup in use; nevertheless, because we intended to apply the fitting method also to time-resolved transmittance curves for which Eq. (1) does not hold, we were forced to choose this approach. In the case of reflectance measurements, we can greatly ease the library buildup since the library curves can be generated for the desired ρ and τ by applying Eq. (1) if all the individual photon histories have been recorded (as in Ref. 10). Compared with the method presented by Kienle and Patterson,[11] our approach is less accurate (they showed an error of $<3\%$, although only on simulations). On the other hand, it has a wider applicability and does not require a rather critical interpolation of the library curves in the time domain.

7. Conclusions

We have tested a fast method to analyze time-resolved reflectance or transmittance distributions with a library of Monte Carlo simulations. Compared with the solution of the diffusion equation, the method improves the accuracy of the fitting of both $\mu_s{}'$ and μ_a for a small distance between the injection and the collection fibers and for low scattering values. The method requires an *a priori* assumption on the *g* value, although a limited discrepancy between the real *g* and the assumed one causes little changes on the fitted $\mu_s{}'$.

References

1. M. S. Patterson, B. Chance, and B. C. Wilson, "Time resolved reflectance and transmittance for the noninvasive measurement of tissue optical properties," Appl. Opt. **28,** 2331–2336 (1989).
2. S. L. Jacques, "Time resolved reflectance spectroscopy in turbid tissues," IEEE Trans. Biomed. Eng. **36,** 1155–1161 (1989).
3. B. C. Wilson and S. L. Jacques, "Optical reflectance and transmittance of tissues: principles and applications," IEEE J. Quantum Electron. **26,** 2186–2199 (1990).
4. S. J. Madsen, B. C. Wilson, M. S. Patterson, Y. D. Park, S. L. Jacques, and Y. Hefetz, "Experimental tests of a simple diffusion model for the estimation of scattering and absorption coefficients of turbid media from time-resolved diffuse reflectance measurements," Appl. Opt. **31,** 3509–3517 (1992).
5. R. Cubeddu, M. Musolino, A. Pifferi, P. Taroni, and G. Valentini, "Time resolved reflectance: a systematic study for the application to the optical characterization of tissue," IEEE J. Quantum Electron. **30,** 2421–2430 (1994).
6. K. M. Yoo, F. Liu, and R. R. Alfano, "When does the diffusion approximation fail to describe photon transport in random media?" Phys. Rev. Lett. **64,** 2647–2650 (1990); **65,** 2210–2211 (1990).
7. R. C. Haskell, L. O. Svaasand, T.-T. Tsay, T.-C. Feng, M. S. McAdams, and B. J. Tromberg, "Boundary conditions for the diffusion equation in radiative transfer," J. Opt. Soc. Am. A **11,** 2727–2741 (1994).
8. A. Kienle and M. S. Patterson, "Improved solutions of the steady-state and the time-resolved diffusion equations for reflectance from a semi-infinite turbid medium," J. Opt. Soc. Am. A **14,** 246–254 (1997).
9. A. M. K. Nilsson, R. Berg, and S. Andersson-Engels, "Measurements of the optical properties of tissue in conjunction with photodynamic therapy," Appl. Opt. **34,** 4609–4619 (1995).
10. M. H. Eddowes, T. N. Mills, and D. T. Delpy, "Monte Carlo simulations of coherent backscatter for identification of the optical coefficients of biological tissues *in vivo*," Appl. Opt. **34,** 2261–2267 (1995).
11. A. Kienle and M. S. Patterson, "Determination of the optical properties of turbid media from a single Monte Carlo simulation," Phys. Med. **41,** 2221–2227 (1996).
12. A. Pifferi, R. Berg, P. Taroni, and S. Andersson-Engels, "Fitting of time-resolved reflectance curves with a Monte Carlo model," in *Advances in Optical Imaging and Photon Migration*, Vol. 2 of OSA Trends in Optics and Photonics (Optical Society of America, Washington, D.C., 1996), pp. 311–314.
13. R. F. Bonner, R. Nossal, S. Havlin, and G. H. Weiss, "Model for photon migration in turbid biological media," J. Opt. Soc. Am. A **4,** 423–432 (1987).
14. K. Furutsu and Y. Yamada, "Diffusion approximation for a dissipative random medium and the applications," Phys. Rev. E **50,** 3634–3640 (1994).
15. L. Wang and S. Jacques, "Monte Carlo modeling of light transport in multi-layered tissues in standard C," Rep. (Laser Biology Research Laboratory, M.D. Anderson Cancer Center, University of Texas, 1515 Holcombe Boulevard, Houston, Tex., 1992).
16. R. Berg, "Laser-based cancer diagnosis and therapy—tissue optics considerations," Ph.D. dissertation (Division of Atomic Physics, Lund Institute of Technology, Lund, Sweden, 1995).
17. L. S. Lasdon, A. D. Waren, A. Jain, and M. Ratner, "Design and testing of a generalized reduced gradient code for nonlinear programming," ACM Trans. Math. Software **4,** 34–50 (1978).